Acta Chemica Scandinavica A 39 (1985) 241–257

Thermodynamics of Molten Mixtures of Na_3AlF_6—Al_2O_3 and NaF—AlF_3

A. STERTEN and I. MÆLAND

Institutt for teknisk elektrokjemi, NTH, Universitetet i Trondheim,
N-7034 Trondheim-NTH, Norway

Emf data of the concentration cell

$Al|Na_3AlF_6(l), Al_2O_3$ (sat)| $|Na_3AlF_6(l), Al_2O_3|Al$

were combined with thermodynamic data from the literature to give consistent activity data of NaF, AlF_3, $NaAlF_4$ and Na_3AlF_6 as a function of temperature and composition in the system Na_3AlF_6-Al_2O_3. Corresponding activity data in the NaF-AlF_3 system were also derived. The Gibbs energy change for the following reactions was derived:

$3NaF(l)+AlF_3(s)=Na_3AlF_6(l)$; $\Delta G°=-45{,}000-54.135T$ J

$5NaF(l)+3AlF_3(s)=Na_5Al_3F_{14}(l)$; $\Delta G°=1{,}660-218.2T$ J

$NaF(l)+AlF_3(s)=NaAlF_4(l)$; $\Delta G°=26{,}060-73.5T$ J

$NaF(l)+AlF_3(s)=NaAlF_4(g)$; $\Delta G°=187{,}100-173.2T$ J

The standard enthalpy of formation of liquid Na_3AlF_6 from its elements at 298 K is derived to be $-3\,249.600\pm4$ kJ/mol. The cryolite liquidus line in the Na_3AlF_6-Al_2O_3 system was reproduced using the heat of melting $\Delta H°_m=106.745$ kJ/mol. The calculations support the idea of some solid solution of AlF_3 in Na_3AlF_6 at temperatures close to the melting point.

Activity data of NaF, AlF_3, $NaAlF_4$ and Na_3AlF_6 as a function of temperature and composition in NaF-AlF_3 melts saturated with alumina were recently published.[1] The activities of NaF and AlF_3 as a function of the mol ratio $r=n_{NaF}/n_{AlF_3}$ were described by the following empirical equations

$r^*<r<1.24$

$$\ln a_{AlF_3}=\frac{F}{RT}\left[1.361\ \ln\frac{(3+r)(0.3+0.9r^*)}{(3+r^*)(0.3+0.9r)}+0.9r^*-0.9r+2.7\ \ln\frac{(3+r)}{(3+r^*)}\right] \quad (1)$$

$1.24<r<15$

$$\ln a_{AlF_3}=\frac{F}{RT}\left[1.361\ \ln\frac{(3+r)}{(0.3+0.9r)}-1.493\right]+\ln a_{AlF_3}(r=1.24) \quad (2)$$

$15>r>1.24$

$$\ln a_{NaF}=\frac{F}{RT}\left[3.63\ln r+0.454\ln(3+r)-4.084\ln(0.3+0.9r)-0.423\right]-0.106 \quad (3)$$

0302-4377/85 $2.50

$1.24>r>r^*$

$$\ln a_{NaF}=\frac{F}{RT}\left[3.63\ln r+1.354\ln(3+r)-4.084\ln(0.3+0.9r)-1.724\right]-0.106 \quad (4)$$

where r^* is the NaF/AlF_3 mol ratio of a melt saturated with both AlF_3 and Al_2O_3. The last term in eqn. (2) is the natural logarithm of the activity of AlF_3 at $r=1.24$ to be computed from eqns. (1) and (5)

$$T(K)=3282\ln\left[\frac{0.3}{r^*}+0.9\right]-271.2r^*+801 \quad (5)$$

Eqn. (5) expresses the relationship between r^* and T.

The standard states of the activities are liquid NaF and solid AlF_3. It should be emphasized that eqns. (1)–(4) are valid only for NaF—AlF_3 melts saturated with alumina in the temperature range between the univariant liquidus curves in the system and about 1300 K as the upper limit. The error limits were estimated to be within ±5 % of the numerical values calculated from eqns. (1)–(4). Activity data of Yoshida and Dewing[2] and of Kvande[3] deviate slightly from those calculated from eqns. (1)–(4). This point is further discussed below.

As regards the system Na_3AlF_6—Al_2O_3 there are relatively few published activity data. The activity of Na_3AlF_6 as a function of the oxide content can be estimated from data for the liquidus curve describing equilibrium reaction [eqn. (6)] and the corresponding cryoscopic equation. This procedure is discussed below in view of some solid solubility of AlF_3 in cryolite as demonstrated by Dewing.[4,5]

$$Na_3AlF_6(s)=Na_3AlF_6(l) \quad (6)$$

The present communication gives activity values of NaF, AlF_3, $NaAlF_4$ and Na_3AlF_6 as a function of temperature and composition for liquid mixtures of Na_3AlF_6 and Al_2O_3. The final data are derived by a "trial and error" treatment of emf data of cell [I]

$$Al|Na_3AlF_6,\ Al_2O_3(sat)|\ |Na_3AlF_6,\ Al_2O_3(x)|Al \quad [I]$$

and the more reliable literature data describing the system. A similar consistent thermodynamic description of the NaF—AlF_3 binary system is also presented.

The activity data derived were fitted to equations of the type

$$\ln a=(A/T)+B \quad (7)$$

where A and B are considered to be temperature independent constants for a given melt composition. The validity of this assumption may be questionable particularly since the standard state for the activity of AlF_3 is the solid compound. However, the available data did not permit a more accurate evaluation of eqn. (7). The relationship between activities described by eqn. (7) and partial molar quantities is as given by eqns. (8)–(10).

$$\Delta\bar{G}=RT\ln a=RA+RBT \quad (8)$$

$$\Delta\bar{H}=\frac{\partial(\Delta\bar{G}/T)}{\partial(1/T)}=RA \tag{9}$$

$$\Delta\bar{S}=(\Delta\bar{H}-\Delta\bar{G})/T=-RB \tag{10}$$

EXPERIMENTAL

A lot of experimental work was done in order to obtain a satisfactory design of the cell [I] since it turned out to be difficult to establish reliable emf readings. However, a cell performance as indicated in Fig. 1 gave usually reproducible emf values. The half cell with the reference melt, *i.e.* liquid Na_3AlF_6 saturated with solid Al_2O_3 and the Al electrode, was contained in a closed alumina tube. The micro pores in the tube wall are wetted by the liquid mixture. This reference compartment was placed inside a crucible made of BN also containing Na_3AlF_6 saturated with Al_2O_3. This electrolyte also penetrates the wall of the BN crucible establishing electrolytic contact between the electrodes. The Al electrode in the outer compartment, H in Fig. 1, consisted of a hot dipped aluminium coating (700 °C) on a tantalum wire. A similar electrode has previously been applied by Yoshida and Dewing.[2] The addition of α-Al_2O_3 to the melt in the outer compartment was made through an alumina tube (not shown in Fig. 1). The cell arrangement was located inside a closed tube furnace in an argon atmosphere. The temperature of the cell was measured with a calibrated Pt-Pt 10 % Rh thermocouple.

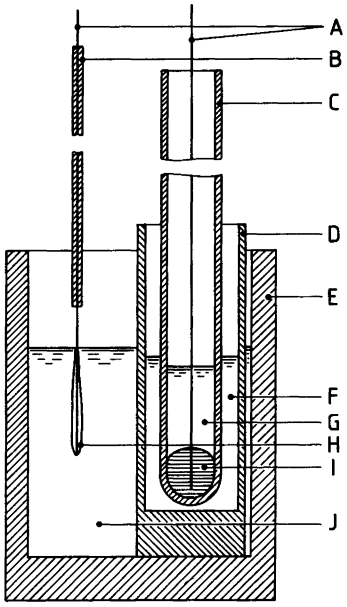

Fig. 1. Cell design. A Tantalum wire, B Alumina protection tube, C Alumina tube crucible, D BN crucible, E Graphite crucible, F Cryolite saturated alumina melt, G Cryolite saturated alumina melt, H and I Al electrodes, J Cryolite alumina melt.

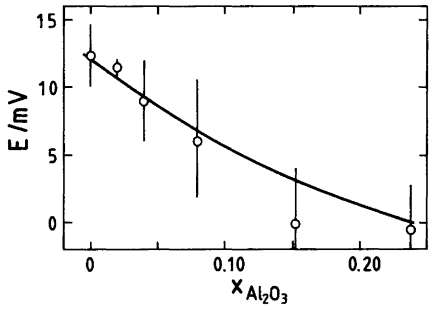

Fig. 2. Emf of cell [I] (see text) as a function of the Al_2O_3 mol fraction in Na_3AlF_6(l) at 1285 K.

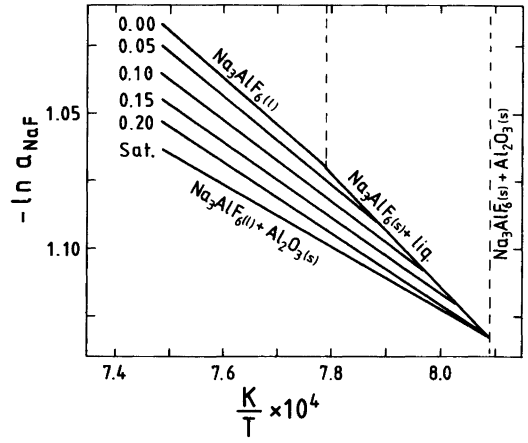

Fig. 3. The negative natural logaritm of the activity of NaF in the Na_3AlF_6—Al_2O_3 system as a function of reciprocal temperature. The numbers in the figure denote the mol fraction of alumina in the melt. The standard state with unit activity is liquid NaF.

RESULTS AND COMMENTS

The alumina content in the right hand side compartment of cell [I] was successively increased to saturation. Except in some preliminary runs the potential of the cell was found to be E=O ±4 mV at saturation. This means that both aluminium electrodes gave reproducible emf values and that the melt compositions in the two half cells were almost identical at the end of each run. Average values of the cell potential with standard deviations as a function of the oxide content are indicated in Fig. 2. The emf of the cell was found to be independent of temperature in the range 1285–1325 K within the experimental uncertainly of ±4 mV. The fully drawn curve in Fig. 2 is discussed below.

The emf of cell [I] can be written as eqn. (11)

$$E=-\frac{RT}{3F}\ln\left[\frac{a_{AlF_3(*)}}{a_{AlF_3}}\right]\left[\frac{a_{NaF}}{a_{NaF(*)}}\right]^3 \qquad (11)$$

if the transference number of the sodium ions through the membranes shown in Fig. 1 is taken equal to unity. The possible error thereby introduced is believed to be only of minor importance.[1] The sign(*) refers to the left hand side reference compartment. The corresponding activities can be computed from eqns. (1)–(5). Measured emf data shown in Fig. 2, combined with eqn. (11) do not allow separate NaF and AlF_3 activities to be

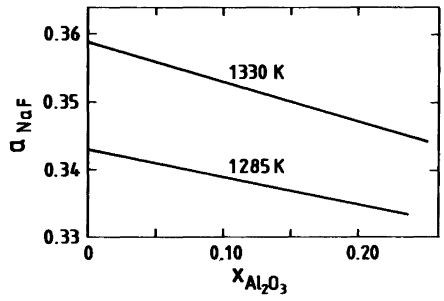

Fig. 4. The activity of NaF as a function of the Al_2O_3 mol fraction dissolved in Na_3AlF_6(l).

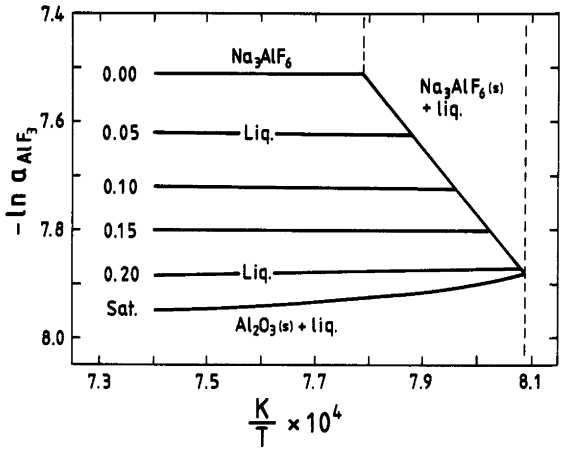

Fig. 5. The negative natural logarithm of AlF_3 as a function of reciprocal temperature in the system Na_3AlF_6—Al_2O_3. The numbers in the figure denote the mol fraction of dissolved Al_2O_3 in the melt. The standard state with unit activity is solid AlF_3.

calculated. These data should then be combined with some other relevant literature values of the system Na_3AlF_6—Al_2O_3.

The data derived below are based on a correlation of the emf data given above, the activity data given in eqns. (1)–(5)[1] integral heat of mixing data from Hong and Kleppa,[7] partial molar heat of mixing data of Na_3AlF_6 in Na_3AlF_6—Al_2O_3-melts from Holm,[8] the cryolite liquidus curve and the heat of melting of Na_3AlF_6 from different sources and vapour pressure data from Kvande[3] and Kuxmann and Tillessen.[17] The "trial and error" procedure used to derive activity data is in fact unimportant and will not be described. However, the derived data will be discussed in view of the requirement of internal consistency.

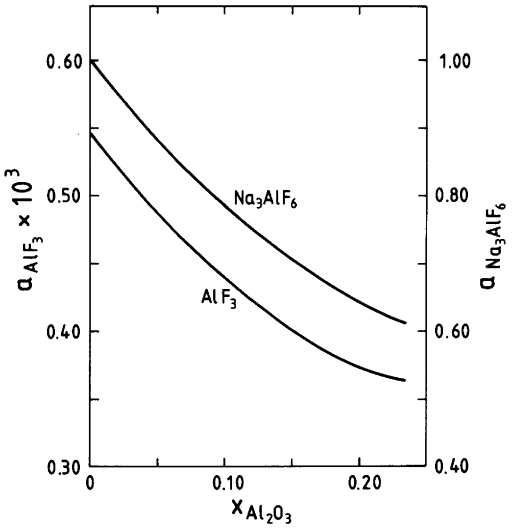

Fig. 6. The activities of AlF_3 and Na_3AlF_6 as a function of Al_2O_3 dissolved in liquid Na_3AlF_6 at 1285 K. The standard states with unit activities are solid AlF_3 and liquid Na_3AlF_6.

THE BINARY SYSTEM Na_3AlF_6-Al_2O_3

Thermodynamic data of NaF(l), AlF_3(s), Na_3AlF_6(l) and $NaAlF_4$(l). Derived activities of NaF, AlF_3, Na_3AlF_6 and $NaAlF_4$ are given in Table 1, while graphical presentations are shown in Figs. 3–6. The given data for $NaAlF_4$ are discussed below. It should be noted that the variation of the activity of NaF with composition for a given temperature is very small. On the other hand there is a marked decrease in the activities of AlF_3 and of Na_3AlF_6 with increasing alumina content which can be seen by comparison of Figs. 4 and 6.

Results given in Table 2 show that the present work is in complete agreement with eqns. (2)–(4) from Sterten *et al.*[1] Other literature values[2,3,6] show some minor deviations from the present work.

From Table 1 and eqn. (9) partial molar heat of mixing values are derived as $\Delta\bar{H}_{NaF}=-14.44$ kJ/mol and $\Delta\bar{H}_{AlF_3}=1.66$ kJ/mol for pure liquid cryolite. Fig. 7 shows integral heat of mixing values of solid AlF_3 with liquid NaF from a work of Hong and Kleppa.[7] The tangent to the curve at the cryolite composition gives intercepts values in

Table 1. Activity data of NaF, AlF_3, $NaAlF_4$ and Na_3AlF_6 in liquid mixtures of Na_3AlF_6–Al_2O_3 given by A and B in the equation $\ln a=(A/T)+B$, where $\ln a$ is the natural logarithm of the activity at different mol fractions (x) of Al_2O_3 in the temperature range between the liquidus and about 1300 K. The standard states with unit activities are pure liquid NaF, solid AlF_3, liquid Na_3AlF_6 and liquid $NaAlF_4$. The uncertainty is estimated to be less than 10 % of the numerical value of the activity.

	NaF(l)		AlF_3(s)		Na_3AlF_6(l)		$NaAlF_4$(l)	
$x_{Al_2O_3}$	*A*	*B*	*A*	*B*	*A*	*B*	*A*	*B*
0.000	−1737	0.283	−200	−7.360	0	0.000	−5071	1.763
0.025	−1714	0.262	−200	−7.422	70	−0.125	−5043	1.680
0.050	−1657	0.215	−200	−7.471	240	−0.315	−4991	1.584
0.075	−1584	0.155	−200	−7.523	460	−0.547	−4918	1.472
0.10	−1514	0.097	−180	−7.583	690	−0.781	−4828	1.354
0.15	−1400	0.003	− 60	−7.757	1150	−1.237	−4594	1.086
0.20	−1310	−0.073	+170	−8.006	1650	−1.714	−4274	0.761
0.25	−1240	−0.134	+510	−8.327	2200	−2.218	−3864	0.379

Table 2. Comparison of activity data of NaF and AlF_3 in pure liquid Na_3AlF_6 and in liquid Na_3AlF_6 saturated with α-Al_2O_3 from different sources. The standard states are pure liquid NaF and solid AlF_3.

Composition	Ref.	a_{NaF}	a_{AlF_3}	*T*/K
Na_3AlF_6	Dewing[6]	0.43	0.40×10^{-3}	1293
	Kvande[3]	0.38±0.04	$(0.8\pm0.1)\times10^{-3}$	1300
	This work	0.349±0.015	$(0.55\pm0.03)\times10^{-3}$	1300
Na_3AlF_6	Yoshida *et al*[2]	0.31	0.58×10^{-3}	1273
Al_2O_3(sat)	Kvande[3]	0.30±0.01	0.5×10^{-3}	1300
	Sterten *et al*[1]	0.34±0.015	$(0.36\pm0.02)\times10^{-3}$	1300
	This work	0.341±0.015	$(0.36\pm0.02)\times10^{-3}$	1300

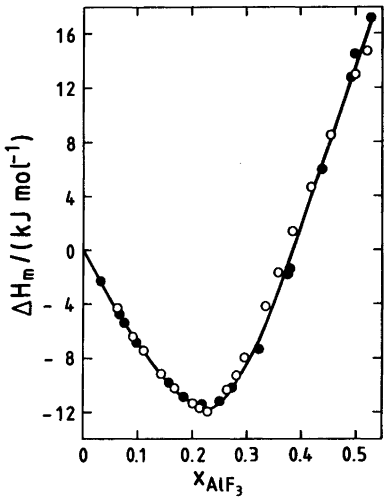

Fig. 7. Integral heat of mixing of solid AlF_3 in liquid NaF as a function of the mol fraction of dissolved AlF_3 at 1298 K. ● Experimental points from Hong and Kleppa.[7] ○ Present work.

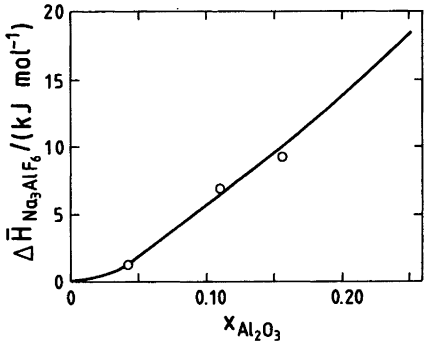

Fig. 8. Partial heat of mixing values for Na_3AlF_6 as a function of the mol fraction of Al_2O_3 in the system Na_3AlF_6—Al_2O_3 for temperatures in the range between the liquidus and ≃1300 K. ○ Experimental points from Holm.[8] The line represents the present work.

complete agreement with the partial molar quantities derived above. Points describing the present work are discussed below.

The fully drawn curve in Fig. 2 is calculated from eqn. (11) using activity data in Table 1. The figure shows satisfactory agreement between the experimental points and the calculated curve.

Fig. 8 shows partial molar heat of mixing data for Na_3AlF_6 in the $Na_3AlF_6-Al_2O_3$ system. The fully drawn curve is calculated from eqn. (9) using the data in Table 1. The curve is in agreement with experimental data given by Holm[8] and Julsrud.[9]

The standard Gibbs energy change associated with reaction (12) is properly described by eqn. (13) based on the activity data in Table 1 for all the melt compositions given in the temperature range from 1230 to 1300 K.

$$3NaF(l)+AlF_3(s)=Na_3AlF_6(l) \quad (12)$$

$$\Delta G^\circ(12)=-45\,000-54.135T\ J \quad (13)$$

This means that all the activity data for NaF, AlF_3 and Na_3AlF_6 in Table 1 are internally consistent. The uncertainty in the Gibbs energy is estimated to ±2 kJ.

Eqn. (13) deviates slightly from the corresponding equation (14) obtained from the JANAF tables.[10]

$$\Delta G^\circ(12)=-43\,325-47.074T\ J \quad (14)$$

Table 3 shows that $\Delta H^\circ_{298}=-100.6\ \pm0.3$ kJ for reaction (12) fits the JANAF[10] free energy function and the Gibbs energy eqn. (13) of the present work for temperatures far

Table 3. Standard enthalpy change ΔH°_{298} for the reaction $3NaF(l)+AlF_3(s)=Na_3AlF_6(l)$. The values are calculated by use of the free energy function $(\Delta G^\circ-\Delta H^\circ_{298})/T$ from the JANAF tables[10] and the Gibbs energy eqn. (13) from the present work.

T	$(\Delta G^\circ-\Delta H^\circ_{298})/T$	ΔG°	$\Delta G^\circ-\Delta H^\circ_{298}$
K	J/K	kJ	kJ
1300	11.468	−115.376	−100.467
1400	14.242	−120.789	−100.850
1500	17.041	−126.203	−100.641

above the cryolite melting point 1284 K. The corresponding value using data only from the JANAF tables[10] is $\Delta H^\circ_{298}=-89.609$ kJ. It is believed that the major part of the discrepancy is related to the standard enthalpy of formation of $Na_3AlF_6(l)$ from its elements at 298 K. Accepting this explanation the new value turns out to be,

$$\Delta H^\circ_{f298}[Na_3AlF_6(l)]=-3249.600\pm4 \text{ kJ/mol} \quad (15)$$

which is 10.990 kJ more negative than the corresponding JANAF[10] value. This means that the standard Gibbs energy and enthalpy of formation data for $Na_3AlF_6(l)$ given in the JANAF tables should be corrected by exactly that amount. Data corrected in this manner are included in Table 4, together with some other data to be discussed below. It should be noted that the Gibbs energy of formation of $Na_3AlF_6(l)$ in this table are in agreement with eqn. (13).

The cryolite liquidus curve and the heat of melting. In a previous work[1] the Gibbs energy change of reaction (16)

$$Na_3AlF_6(s)=3NaF(l)+AlF_3(s) \quad (16)$$

was given as eqn. (17)

$$\Delta G^\circ(16)=151\,745-29.0T \text{ J} \quad (17)$$

The Gibbs energy change, [eqn. (18)], associated with reaction (6) is found from eqns. (13) and (17).

Table 4. Standard thermodynamic data of $Na_3AlF_6(l)$ and $Na_5Al_3F_{14}(l)$ derived from the present data and the JANAF tables.[10] See text.

	$Na_3AlF_6(l)$		$Na_5Al_3F_{14}(l)$	
T/K	$-\Delta H^\circ_f$ kJ mol^{-1}	$-\Delta G^\circ_f$ kJ mol^{-1}	$-\Delta H^\circ_f$ kJ mol^{-1}	$-\Delta G^\circ_f$ kJ mol^{-1}
900	3223.235	2795.195		
1000	3217.327	2747.757	7245.450	6288.846
1100	3200.729	2701.624	7228.660	6194.054
1200	3476.120	2651.215	7698.757	6091.057
1300	3457.242	2583.234	7678.896	5957.939
1400	3438.418	2516.712	7659.344	5826.298

$$\Delta G°(6)=106\,745-83.135T\ \text{J} \tag{18}$$

This equation agrees with a melting point of 1284 K for Na_3AlF_6 in complete agreement with observations.

$$\Delta H°_m=106.745\ \text{kJ/mol} \tag{19}$$

Eqn. (19) then gives the heat of melting of Na_3AlF_6. Dewing[5] pointed out that the heat content of solid cryolite exhibits a non-linear temperature dependence as the melting point is approached. This observation may be due to a minor side reaction (20),

$$Na_3AlF_6(s)=2NaF(l)+NaAlF_4(g) \tag{20}$$

taking place during the heating period. Another and more important factor may be a minor solid solubility of AlF_3 in Na_3AlF_6 at higher temperatures.[4,5] Such a solubility will also give rise to a premelting effect, which can explain the temperature dependence of the calorimetric data for temperatures between the $NaF-Na_3AlF_6$ eutectic and the cryolite melting point. The heat of melting given by eqn. (19) is in agreement with calorimetric data[11–13] when they are not corrected for the effect of premelting.[5] The heat of melting obtained by linear extrapolation from temperatures below the $NaF-Na_3AlF_6$ eutectic corresponds to $\Delta H°_m \simeq 115$ kJ/mol. This value is not easy to apply since the degree of solid solubility in cryolite and the corresponding activities are not well established.

The fully drawn curve shown in Fig. 9 is a calculated curve based on cryolite activity data from Table 1 and the cryoscopic eqn. (21).

$$RT \ln [a(l)/a(s)]=\Delta H°_m\,(1-T/T_f) \tag{21}$$

The calculation was performed with $\Delta H°_m=106.745$ kJ/mol and by defining the activity of solid cryolite equal to unity $[a(s)=1]$ at all temperatures. A corresponding standard state was applied when the Gibbs energies of the reactions (16) and (6) were derived. This means that the data are internally consistent, in spite of the fact that the standard state may not be a

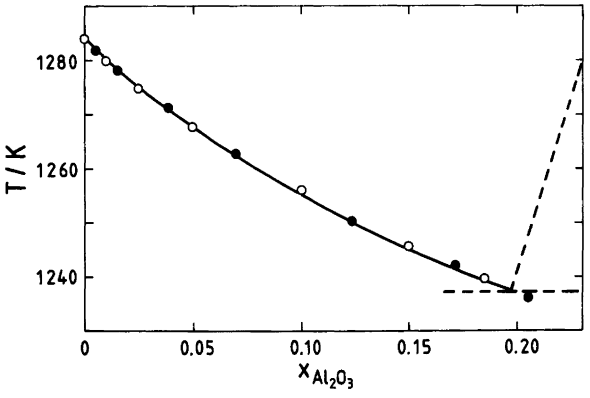

Fig. 9. The liquidus line in the system Na_3AlF_6—Al_2O_3. ●, ○ Experimental points from Holm[14] and Skar[15] respectively. The fully drawn curve is the calculated liquidus line from the present work.

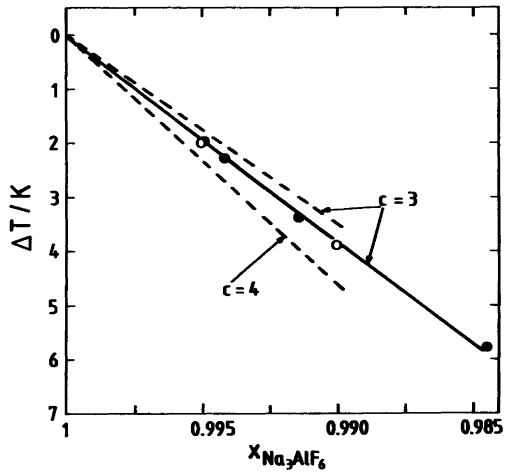

Fig. 10. Freezing point depression in the Na_3AlF_6—Al_2O_3 system. ●, ○ Experimental data from Holm[14] and Skar[15] respectively. The fully drawn curve is the calculated depression using $\Delta H_m^\circ = 106.745$ kJ/mol and $c=3$ (the number of new entities created in the melt by the Al_2O_3 addition). The stipled curves are the calculated depression using $\Delta H_m^\circ = 115$ kJ/mol and $c=3$ and $c=4$.

completely well-defined quantity, since the amount of AlF_3 in solid solution varies with temperature. However, at present it is not possible to use a more precise definition of the standard state. Fig. 9 shows that the calculated liquidus curve from eqn. (21) is in excellent agreement with the experimental liquidus data of Holm[14] and Skar.[15]

$$\Delta T = \frac{RTT_f c x_{Al_2O_3}}{\Delta H_m^\circ \, (x_{Na_3AlF_6} + c x_{Al_2O_3})} \tag{22}$$

Eqn. (21) can be transformed to eqn. (22) for small additions of Al_2O_3. ΔT is the freezing point depression, while c is the number of foreign species created during the alumina addition. Fig. 10 shows that there is nearly complete agreement between experimental points from Holm[14] and Skar[15] and the calculated depression using $\Delta H_m^\circ = 106.745$ kJ/mol and $c=3.0$ species. However, using $\Delta H_m^\circ = 115.000$ kJ/mol the number of foreign species at infinite dilution turns out to lie between three and four which can hardly be correct.

THE BINARY SYSTEM NaF–AlF_3

Table 5 shows the activity data for NaF, AlF_3, Na_3AlF_6 and $NaAlF_4$ in the NaF–AlF_3 binary system. When deriving these data we tried to correlate informations from a number of sources, such as calorimetric measurements of Hong and Kleppa[7] and Holm[16], vapour pressure data of Kvande[3] and Kuxmann and Tillessen[17], the corresponding activity data for melts saturated with alumina, eqns. (1)–(5), from which thermodynamic data for Na_3AlF_6(s) and $Na_5Al_3F_{14}$(s) were derived[1] and finally the data for the Na_3AlF_6–Al_2O_3 system derived above.

Fig. 7 shows that the heat of mixing calculated from the activity data are in satisfactory agreement with experimental data given by Hong and Kleppa.[7] The partial heats of mixing

Table 5. Activity data of NaF, AlF_3, Na_3AlF_6 and $NaAlF_4$ in the liquid binary system $NaF-AlF_3$ expressed by A and B in the equation $\ln a=(A/T)+B$, where $\ln a$ is the natural logaritm of the activity at different mol ratios of NaF and AlF_3 (r=NaF/AlF_3) in the temperature range between the liquidus line and about 1300 K. The standard states with unit activities are liquid NaF, solid AlF_3, liquid Na_3AlF_6 and liquid $NaAlF_4$. The uncertainty is estimated to be less than 10 % of the numerical value of the activity.

	NaF(l)		AlF_3(s)		Na_3AlF_6(l)		$NaAlF_4$(l)	
r	$-A$	B	A	$-B$	$-A$	B	$-A$	B
15.0	0	−0.073	−8400	6.508	2988	−0.216	11534	+2.259
10.0	80	−0.080	−7700	6.151	2528	+0.120	10914	+2.609
8.0	150	−0.094	−7000	6.050	2038	+0.179	10284	+2.696
6.0	300	−0.115	−6020	5.765	1508	+0.401	9454	+2.960
5.0	500	−0.090	−4930	5.947	1018	+0.294	8564	+2.803
4.0	920	+0.012	−3200	6.378	550	+0.169	7254	+2.564
3.7	1100	+0.074	−2600	6.560	488	+0.173	6834	+2.354
3.4	1340	+0.153	−1800	6.800	408	+0.170	6274	+2.193
3.0	1737	+0.283	− 200	7.360	0	0.000	5071	+1.763
2.8	2020	+0.378	+ 950	7.896	−312	−0.314	4204	+1.322
2.6	2350	+0.471	+2100	8.480	−462	−0.556	3384	+0.831
2.4	2700	+0.608	+3250	9.070	−562	−0.735	2584	+0.378
2.2	3100	+0.718	+4400	9.533	−512	−0.868	1834	+0.025
2.0	3500	+0.789	+5500	9.835	−412	−0.957	1134	−0.206
1.8	4000	+0.877	+6630	10.104	− 42	−0.962	504	−0.387
⅔	4400	+0.947	+7400	10.326	388	−0.974	134	−0.539
1.6	4600	+0.957	+7800	10.410	588	−1.028	− 66	−0.613
1.4	5300	+0.973	+8800	10.480	1688	−1.052	−366	−0.667
1.2	6200	+0.872	+9700	10.198	3488	−1.071	−366	−0.486
1.0	7300	+0.297	+10430	9.137	6058	−1.735	0	0.000
0.9	8200	+0.093	+10700	8.551	8488	−1.761	634	0.382

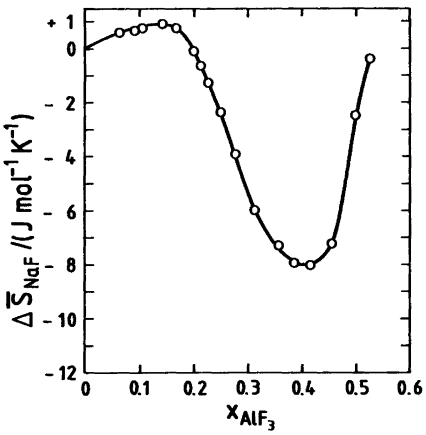

Fig. 11. The partial molar entropy of NaF as a function of AlF_3 mol fraction in the binary system NaF—AlF_3 at 1300 K.

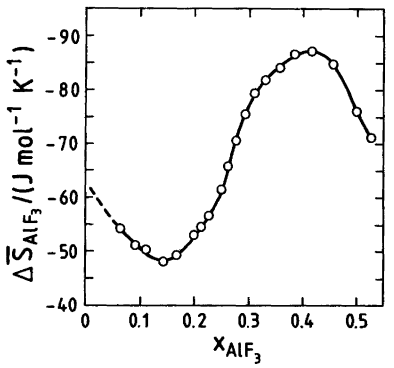

Fig. 12. The partial molar entropy of AlF_3 as a function of the mol fraction of AlF_3 at 1300 K in the system NaF—AlF_3.

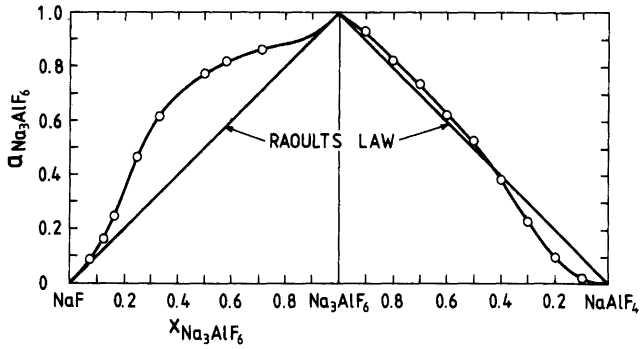

Fig. 13. The activity of Na_3AlF_6 in the systems NaF—Na_3AlF_6 and Na_3AlF_6—$NaAlF_4$ at 1300 K. The points are calculated from data in Table 5.

of NaF and Na_3AlF_6 in NaF–Na_3AlF_6 melts presented by Holm[16] and Julsrud[9] seem to fit nicely to the data given in Table 5.

Fig. 11 shows a plot of $\Delta\bar{S}_{NaF}$ as a function of composition. Hong and Kleppa[7] obtained a similar curve using Gibbs energy data from Dewing.[6,18] Fig. 12 shows a corresponding plot of $\Delta\bar{S}_{AlF_3}$. The curves in both figures have inflection points at the cryolite composition which indicate that this is a composition of maximum local order.[7,19] The shapes of the curves given in Figs. 11 and 12 seem to indicate inflection points also around $x_{AlF_3}=0.50$, which supports the notion of AlF_4^- being a stable complex ion in the system. A more detailed discussion of the structural entities in the system is given elsewhere.[7,9,23]

Figs. 13 and 14 show that the activities of NaF, $NaAlF_4$ and Na_3AlF_6 as expected follow Raoults law as the compostions approach the standard states. It should be noted that the cryolite activity in the NaF–Na_3AlF_6 system shows a demixing tendency. It is difficult to assess the uncertainty in the present activity data. However, the uncertainty will probably not exceed 10 % of the activity values calculated from Table 5. The activities of NaF and AlF_3 given in Table 5 show some minor deviations from corresponding data given by Dewing.[6]

Thermodynamic data for $Na_5Al_3F_{14}$. The Gibbs energy change associated with reaction (23)

$$5NaF(l)+3AlF_3(s)=Na_5Al_3F_{14}(l) \qquad (23)$$

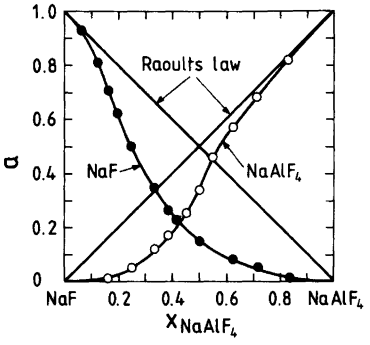

Fig. 14. The activities of NaF and $NaAlF_4$ in the NaF—$NaAlF_4$ system at 1300 K. The points are calculated from data in Table 5.

is well described by eqn. (24) in accordance with the activity data in Table 5.

$$\Delta G°(23)=1660-218.2T\,\mathrm{J} \tag{24}$$

The estimated uncertainty in the Gibbs energy is ±5000 J. In a previous work by Sterten et al[1], the Gibbs energy change corresponding to the reaction (25) was

$$Na_5Al_3F_{14}(s)=5NaF(l)+3AlF_3(s) \tag{25}$$

described by the eqn. (26).

$$\Delta G°(25)=229\,890-6.47T\,\mathrm{J} \tag{26}$$

The Gibbs energy of melting according to eqn. (27)

$$Na_5Al_3F_{14}(s)=Na_5Al_3F_{14}(l) \tag{27}$$

is then easily derived as eqn. (28)

$$\Delta G°(27)=231\,550-224.70T\,\mathrm{J} \tag{28}$$

This corresponds to a hypothetical melting point of 1030.5 K, which seems to fit nicely into the phase diagram data.[1] Eqn. (29) derived from calorimetric data given by Holm[16] agrees reasonably well with eqn. (28).

$$\Delta G°(27)=237\,109-230.091T\,\mathrm{J} \tag{29}$$

Eqn. (24) is combined with thermodynamic data for NaF and AlF_3 from the JANAF tables[10] to give the standard enthalpy and Gibbs energy data for $Na_5Al_3F_{14}$ shown in Table 4. Corresponding data have not previously been published as far as we know.

Thermodynamic data for $NaAlF_4(l)$. The Gibbs energy change of reaction (30)

$$NaF(l)+AlF_3(s)=NaAlF_4(l) \tag{30}$$

is described by eqn. (31),

$$\Delta G°(30)=(26\,060-73.50T)\pm2000\,\mathrm{J} \tag{31}$$

based on data from Table 5, which is in reasonable agreement with the previously published data eqn. (32)[1].

$$\Delta G°(30)=(27\,167-72.83T)\pm4000\,\mathrm{J} \tag{32}$$

The fit is not so good when eqn. (31) is compared with eqn. (33) which was derived from activity data given by Dewing.[6]

Table 6. Standard thermodynamic data of $NaAlF_4(l)$ and $NaAlF_4(g)$ from the present work and the JANAF tables.[10]

	$NaAlF_4(l)$		$NaAlF_4(g)$	
T/K	$-\Delta H_f^\circ$ kJ mol^{-1}	$-\Delta G_f^\circ$ kJ mol^{-1}	$-\Delta H_f^\circ$ kJ mol^{-1}	$-\Delta G_f^\circ$ kJ mol^{-1}
900	2021.100	1788.333	1860.060	1717.023
1000	2027.786	1761.918	1866.746	1700.578
1100	2023.883	1735.532	1862.843	1684.162
1200	2117.328	1707.565	1956.288	1666.165
1300	2112.752	1673.602	1951.712	1642.172
1400	2108.207	1639.991	1947.167	1618.531

$$\Delta G^\circ(29) = 33\,656 - 75.312T \text{ J} \quad (33)$$

Eqn. (31) is combined with data for NaF and AlF_3 from the JANAF tables[10] to give the thermodynamic properties of $NaAlF_4(l)$ given in Table 6.

Eqns. (30) and (31) are combined with activity data for NaF and AlF_3 to give the data for $NaAlF_4(l)$ shown in Table 1. From the table it is found that $a_{NaAlF_4}=0.118$ for $x_{Al_2O_3}=0$ and $a_{NaAlF_4}=0.075$ for $x_{Al_2O_3}=0.25$ at 1300 K. Corresponding activity values given by Kvande[3] are 0.15 ± 0.01 and 0.09. From data given by Dewing[6] it is found that $a_{NaAlF_4}=0.064$ for $x_{Al_2O_3}=0$ which deviates considerably from the other data.

Equilibria in the liquid state. The Gibbs energy changes of the reactions (34) and (35)

$$Na_3AlF_6(l) = 2NaF(l) + NaAlF_4(l) \quad (34)$$

$$Na_5Al_3F_{14}(l) = 2NaF(l) + 3NaAlF_4(l) \quad (35)$$

are expressed by eqns. (36) and (37) based on data in Table 5.

$$\Delta G^\circ(34) = 71\,060 - 19.365T \text{ J} \quad (36)$$

$$\Delta G^\circ(35) = 76\,520 - 2.300T \text{ J} \quad (37)$$

The reasonable values of the entropy terms in these equations should be noted. Both the enthalpy and entropy values indicate that the chiolite ion is less stable than the AlF_4^- and AlF_6^{3-} ions.

SOME LIQUID-GAS PHASE EQUILIBRIA

The Na_3AlF_6–Al_2O_3 vapour system. From available literature data it is reasonable to assume that the vapour above Na_3AlF_6–Al_2O_3 melts consists of $NaAlF_4(g)$ as the main

species and some minor quantities of NaF(g) and the dimer $Na_2F_2(g)$. Fig. 15 shows vapour pressure data[3,17] reduced by the partial pressures of NaF and Na_2F_2 as a function of the NaF(l) and $AlF_3(s)$ activity product. This product was calculated from the activity data given in Table 1. The straight lines through the points and the origin clearly show that a contribution of the dimer $Na_2Al_2F_8(g)$ can be neglected in this range of the system.

It should be noted that the vapour pressure data of Kvande[3] and Kuxmann and Tillessen[17] are in general agreement with data given by Gerlach *et al*[20] and Alivaliollahi *et al.*[21]

The Gibbs energy change of the reaction (38)

$$NaF(l)+AlF_3(s)=NaAlF_4(g) \tag{38}$$

is then derived from the lines in Fig. 15 and found to be well expressed by eqn. (39).

$$\Delta G°(38)=187\,100-173.2T\,J \tag{39}$$

If eqns. (30), (31), (38), (39) are combined it follows that the vaporization reaction [eqn. (40)]

$$NaAlF_4(l)=NaAlF_4(g) \tag{40}$$

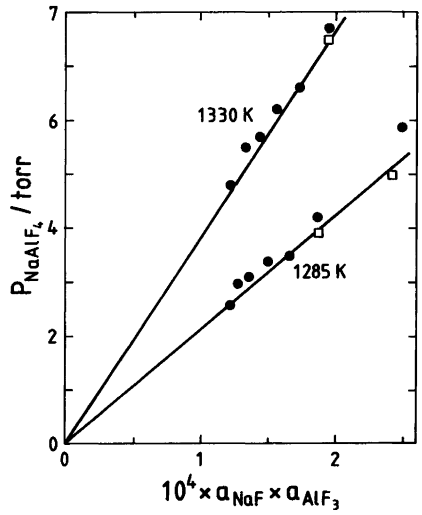

Fig. 15. The experimental points are the total vapour pressure minus the partial pressures of NaF(g) and $Na_2F_2(g)$ above Na_3AlF_6—Al_2O_3 melts as a function of the NaF and AlF_3 activity product. ●, □ Calculated values from Kvande[3] and Kuxmann and Tillessen,[17] respectively. The straight lines are the calculated partial pressure of $NaAlF_4(g)$ from the present work.

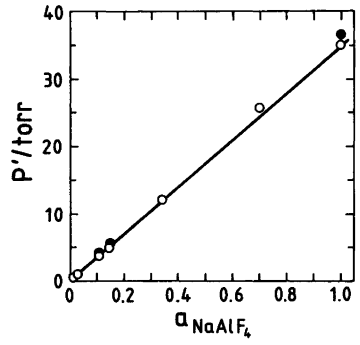

Fig. 16. The experimental points are the total vapour pressure minus the partial pressures of NaF(g), $Na_2F_2(g)$, $AlF_3(g)$ and $Al_2F_6(g)$ above NaF—AlF_3 melts as a function of the activity of $NaAlF_4$. ●, ○ Calculated values from Kvande[3] and Kuxmann and Tillessen,[17] respectively. The straight line is the calculated partial pressure of $NaAlF_4(g)$ from the present work. Temperature: 1285 K.

is described by eqn. (41). The reasonable value of the entropy term should be noted.

$$\Delta G°(40) = 161\,040 - 99.7T \text{ J} \tag{41}$$

Eqn. (41) is also in agreement with a corresponding equation given by Kvande.[3] Thermodynamic data for $NaAlF_4(g)$ are given in Table 6. These data deviate considerably from those given in the JANAF tables[10], which need to be revised as pointed out by Grjotheim *et al.*[22]

The vapour above NaF–NaAlF₄ melts. The vapour pressure P' defined by eqn. (42) is plotted as a function of the activity of $NaAlF_4$ in Fig. 16.

$$P' = P_t - P_{NaF} - P_{Na_2F_2} - P_{AlF_3} - P_{Al_2F_6} \tag{42}$$

P_t is the total vapour pressure in the $NaF-NaAlF_4$ system as determined by Kvande[3] and Kuxmann and Tillessen.[17] The partial vapour pressures of $NaF(g)$, $Na_2F_2(g)$, $AlF_3(g)$ and $Al_2F_6(g)$ are calculated from the activity data in Table 5 and Gibbs energy data from the JANAF tables.[10] The straight line drawn in Fig. 16 represents the partial pressure of $NaAlF_4(g)$ calculated from the eqns. (40) and (41). The differences between the points and the line are rather small, which indicate that the amount of the dimer $Na_2Al_2F_8(g)$ is small even at the $NaAlF_4$ melt composition.

Acknowledgement. Financial support from the Royal Norwegian Council for Scientific and Industrial Research is acknowledged.

REFERENCES

1. Sterten, A., Hamberg, K. and Mæland, I. *Acta. Chem. Scand. A 36* (1982) 329.
2. Yoshida, K. and Dewing, E.W. *Met. Trans. 3* (1972) 683.
3. Kvande, H. *Thermodynamics of the System NaF–AlF₃–Al₂O₃–Al,* Diss., University of Trondheim, NTH, Trondheim 1979.
4. Dewing, E.W. *Met. Trans. 3* (1972) 2699.
5. Dewing, E.W. *Met. Trans. B 9* (1978) 687.
6. Dewing, E.W. *Met. Trans. 3* (1972) 495.
7. Hong, K.C. and Kleppa, O.J. *J. Phys. Chem. 82* (1978) 176.
8. Holm, J.L. *Thermodynamic Properties of Molten Cryolite and Other Fluoride Mixtures,* Diss., University of Trondheim, NTH, Trondheim 1971.
9. Julsrud, S. *Some Oxy-Anion Complexes in Alkali-Fluoride Melts,* Diss., University of Trondheim, NTH, Trondheim 1983.
10. Stull, D.R. and Prophet, H. *JANAF: Thermochemical Tables,* 2nd Ed., NSRDS–NBS 37, Washington 1971.
11. Frank, W.B. *J. Phys. Chem. 65* (1961) 2081.
12. O'Brien, C.J. and Kelley, K.K. *J. Am. Chem. Soc. 79* (1957) 5616.
13. Holm, B.J. and Grønvold, F. *Acta. Chem. Scand. 27* (1973) 2043.
14. Holm, J.L. *Undersøkelser av struktur og faseforhold for en del systemer med tilknytning til aluminiumindustrien,* Diss., University of Trondheim, NTH, Trondheim 1963.
15. Skar, O. *Liquiduskurver i kryolittsmelter ved tilsats av oksyder,* Diss., University of Trondheim, NTH, Trondheim 1981.
16. Holm, J.L. *High Temp. Sci. 6* (1974) 16.
17. Kuxmann, U. and Tillessen, U. *Erzmetall 20* (1967) 147.

18. Dewing, E.W. *J. Electrochem. Soc. 123* (1976) 1289.
19. Østvold, T. *High Temp. Sci. 4* (1972) 51.
20. Gerlach, J., Hennig, U. and Mucke, M. *Erzmetall 26* (1973) 496.
21. Alivaliollahi, M., Gerlach, J. and Hennig, U. *Erzmetall 31* (1978) 220.
22. Grjotheim, K., Motzfeldt, K. and Rao, D.B. *Light Metals 1971, Proc., 100 AIME Annual Meeting,* New York 1971, p. 223.
23. Sterten, A. *Electrochim. Acta 25* (1980) 1673.

Received August 5, 1984.